ACS APPLIED MATERIALS & INTERFACES

Research Article

www.acsami.org

Ultrathin Polymer Films for Transparent Electrode Applications Prepared by Controlled Nucleation

Pejman Hojati-Talemi,[†] Curdin Bächler,[†,‡] Manrico Fabretto,*[,†] Peter Murphy,[†] and Drew Evans[†]

[†]Mawson Institute, University of South Australia, Mawson Lakes, 5095, Australia

[‡]Swiss Federal Institute of Technology (ETH), Department of Materials, Polymer Technology Group, Zurich CH-8093, Switzerland

Supporting Information

ABSTRACT: The vacuum vapor phase polymerization (VPP) technique is capable of producing conducting polymer films with conductivities up to 3400 S cm^{-1}. However, the method is not able to produce robust nano-thin films as required for transparent conducting electrode (TCE) applications. We show that with the addition of aprotic solvents or chelating agents to the oxidant mixture, it is possible to control the polymerization rate, and nucleation, in the VPP process. This provides the opportunity of altering the grain size and depositing conducting polymer films with a thickness of 16 to 200 nm with resulting optical transmission within the range 50−98% that are robust enough to endure the post polymerization processing steps. The figure of merit (FoM), which is used to quantify a film's suitability for TCE applications, results in values from 12 to 25. This result indicates that the nano-films outperform most of the previously reported graphene films and approaches the accepted industry standard for TCE applications.

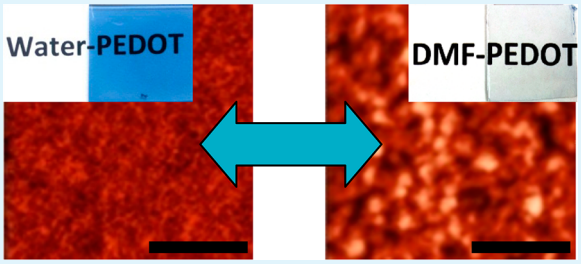

KEYWORDS: *conducting materials, thin films, nanostructures, vapor phase polymerization, PEDOT*

1. INTRODUCTION

The use of transparent conducting electrodes (TCEs) is ubiquitous and forms the basis of many modern optoelectronic devices with some examples being touch-panels,[1] electrochromic display devices,[2] organic light emitting diodes (OLEDs),[3] and solar cells.[4] These electrodes are typically fabricated as a thin film, of a given material, which possesses both high transparency and high electrical conductivity (low sheet resistance). Some example materials currently being investigated for use as TCEs are indium tin oxide (ITO),[5] metal doped zinc oxide,[6] graphene,[7−11] and conducting polymers.[12−17] Among these, ITO has been the most successful option in finding its way into commercial devices, accounting for over 90% of the market. As a result, demand for indium has steadily increased since the early 2000s leading to an order of magnitude increase in its price by 2005.[18]

In order to provide a "standard" across different technologies and materials for the preparation of TCEs, a figure of merit (FoM) has been proposed that includes factors that measure the opto-electrical properties of transparent and conductive thin films.[19,20] This parameter is defined as the ratio of electrical conductivity (σ_{DC}) to optical conductivity (σ_{Op}) and can be calculated using the following equation:[19]

$$\mathrm{FoM} = \frac{\sigma_{DC}}{\sigma_{Op}} = \frac{Z}{2R_s\left(\frac{1}{\sqrt{T}} - 1\right)} \quad (1)$$

where R_s is the sheet resistance, T is the optical transmission, and Z is the impedance of free space (defined as 377 Ω).[19] The accepted minimum industry requirement for a TCE material to replace ITO is a sheet resistance of $R_s \leq 100\ \Omega.\square^{-1}$, coupled with an optical transmission, at 550 nm, of greater than $T \sim 90\%$,[19,21] which yields a FoM greater than 35 when using eq 1.[19] In addition to this well established performance indicator, a new method has recently been developed which monitors the local variation in the FoM (LFoM) across large area TCEs.[22] Such a diagnostic tool may ultimately provide a useful adjunct to the established FoM in determining the overall performance of optoelectronic devices.

In addition to providing an electrical conduction path, the development of consumer electronics in recent years has placed additional requirements on TCE materials, for example, the desire for flexible devices that can be flexed or folded. Therefore, a considerable challenge currently exists in creating materials that are conductive, transparent, and flexible. Under repeated flexing, organic materials such as conducting polymers have been shown to possess sufficient mechanical flexibility such that their optical and electrical performance is not compromised.[23] In addition to acting as a passive conduction path for electrical charge, these polymers can also be utilized as the active layer in many devices such as organic solar cells (OSC),[14,15,17,24] electrochromic displays,[2] OLEDs,[25] and organic field effect transistors (OFETs).[26,27]

Received: July 31, 2013
Accepted: October 23, 2013
Published: October 23, 2013

In order to achieve highly conducting polymer electrodes a variety of approaches have been attempted. Most of the recent research in this area has focused on the chemical treatment of commercially available PEDOT:PSS using different additives such as ionic liquids,[28] various solvents,[15,17] or ethylene glycol.[14] This approach has been able to increase the conductivity of commercially sourced PEDOT:PSS from ∼0.7 $S{\cdot}cm^{-1}$ to ∼2000 $S{\cdot}cm^{-1}$. It has been recently shown that using vacuum vapor phase polymerization in the presence of a structure-directing glycol tri-block copolymer (PEG-PPG-PEG), thin films of poly(3,4-ethylenedioxythiophene) (PEDOT) with electrical conductivities as high as ∼3400 $S{\cdot}cm^{-1}$ can be prepared.[2,29,30] While this process produced low sheet resistances of $R_s \approx 45\ \Omega.\square^{-1}$, the corresponding optical transmission was approximately $T = 80\%$. Substituting these values into eq 1 yields a FoM value of 35.5, a value above the accepted industry requirement of 35.0. Despite this FoM, the films are not deemed transparent enough for use in many opto-electronic devices where an optical transmission of greater than 90% is generally regarded as the accepted minimum.[19] With this film property in mind, an approach for increasing the film's transparency was to control the thickness of the films by simply reducing the polymerization time using previously established protocols.[2,29−31] However, our initial observations indicated that simply reducing the polymerization time to achieve thinner films yielded a concomitant loss in the mechanical robustness of the polymer film, which subsequently fragmented during post-polymerization processing. As a result, an alternate methodology was explored in which the effect of adding aprotic polar solvents or chelating ligands to the oxidant mixture was investigated. The ability of these components to coordinate with Fe(III) centers is well known within the literature,[32−36] and initial observations indicated that this was leading to changes in the redox behavior of the oxidant solution, consequently altering the number of accessible polymerization nucleation sites. A smaller number of nucleation sites can potentially retard the film growth rate. In addition to this, a smaller number of nucleation sites are expected to yield larger polymer grains, thus providing a means to enhanced mechanical properties. As a consequence, this new protocol can be used for producing robust ultrathin films with increased optical transmission.

2. MATERIALS AND METHODS

PEDOT samples were prepared using the vacuum-VPP process, as described previously.[2,31] To prepare the oxidant solutions, the following material ratio was used; a mass ratio of 20:15:30 of 40 wt % Fe(III) Tosylate concentrate solution (CB-40, Clevios) to PEG_{20}-PPG_{70}-PEG_{20} to solvent/polar liquid. The solvent was 1-butanol or ethanol (Aldrich), and the coordinating additive was either deionized water, DMF, NMP, DMSO, or EDTA (ethylenediaminetetraacetic acid disodium salt dihydrate), all supplied from Sigma-Aldrich. All of the materials were used without any further purification. The constituents for all samples are reported in Supporting Information (SI) Table S1.

The conductivity was calculated using $\sigma = (R_s t)^{-1}$, where R_s is the sheet resistance and t is the thickness of the PEDOT film. R_s was measured using a Jandel four point probe, and film thickness was measured using AFM (Integra, NT-MDT). Atomic force microscopy (AFM) imaging was conducted on the same sample over an area of 2.5 × 2.5 μm using non-contact imaging. A HunterLab UltraScan Pro spectrometer was used for measuring transmission across the visible range, and UV−vis spectra of oxidant solutions were acquired by sandwiching a droplet of solution between two quartz slides and using an Agilent Technologies, Cary series UV−Vis−NIR spectrometer. TGA measurements were performed at a heating rate of 10 $°C{\cdot}min^{-1}$ (TA Instruments, 2950). Prior to measuring, the oxidant solution was placed in an aluminum crucible and heated on a hot plate at 70 °C for 3 minutes. This preconditioning was used to mimic the solvent/additive loss which occurs during a typical vacuum-VPP procedure, prior to and during actual polymerization. The surface chemistry of polymer films was analyzed using an SPECS (SAGE, Phoibos 150-HSA) X-ray photoelectron spectroscopy (XPS) system fitted with a non-monochromated Al anode, with a power of 200 W and a base pressure of 2×10^{-6} Pa. Curve fitting was performed with Casa XPS (Neil Fairley, U.K.), using a Shirley linear background. Spectra were charge corrected relative to the aliphatic carbon peak at 285 eV. Cyclic voltammetry was performed using a VoltaLab PGZ100 to analyze the redox properties of oxidant solutions. A standard Ag/AgCl electrode with an ionic liquid interface was used as the reference electrode. Platinum wire has been used as both counter and work electrodes.

3. RESULTS AND DISCUSSION

In the vacuum-VPP process used for the preparation of these films, an oxidant solution of Fe(III)Tosylate (CB-40, Clevios) and tri-block copolymer PEG-PPG-PEG in an ethanol/butanol solvent blend was spin coated on a substrate. The resulting oxidant film was then exposed to a low monomer vapor pressure yielding the growth of the conducting polymer at the oxidant/vapor interface. Although water is not added to the standard oxidant mixture, previous work[30] has demonstrated that the presence of a small concentration of water, carried in the oxidant solution by the tri-block copolymer as a hydration shell, or dissolved within the solvents, or complexed with the Fe(III) tosylate, plays a critical role and is necessary for the formation of PEDOT. Thus, the oxidant solution used in this process is a multi-component mixture where the resulting high conductivity PEDOT film is formed as a consequence of the intricate interplay of competing/complementary mechanisms—from the phase separation of components based on their polarity to the formation of different Fe(III) coordination compounds. When looking at the oxidant itself, in the simple case of hydrated Fe(III), a wide range of iron complexes are reported to exist.[37−40] For the case presented here, the presence of many potential coordinating molecules (such as water, tosylate, ethylene glycol units, and alcohols) in the oxidant solution leads to the possibility of many different complexes being formed. This makes definitive analysis and prediction of those iron complexes imprecise and problematic at best. A review of the literature has shown that these different iron complexes have different redox properties;[37,41] thus, it can be expected that one or more of the Fe(III) complexes present in this multi-component mixture act to nucleate or initiate the polymerization process. This study demonstrates how the addition of coordinating solvents such as dimethylformamide (DMF), N-methyl-2-pyrrolidone (NMP), dimethyl sulfoxide (DMSO), or a chelating ligand such as ethylenediaminetetra-acetic acid (EDTA), can be used to alter the nucleation density and consequently the thickness and optical transmission of the resultant conductive polymer film.

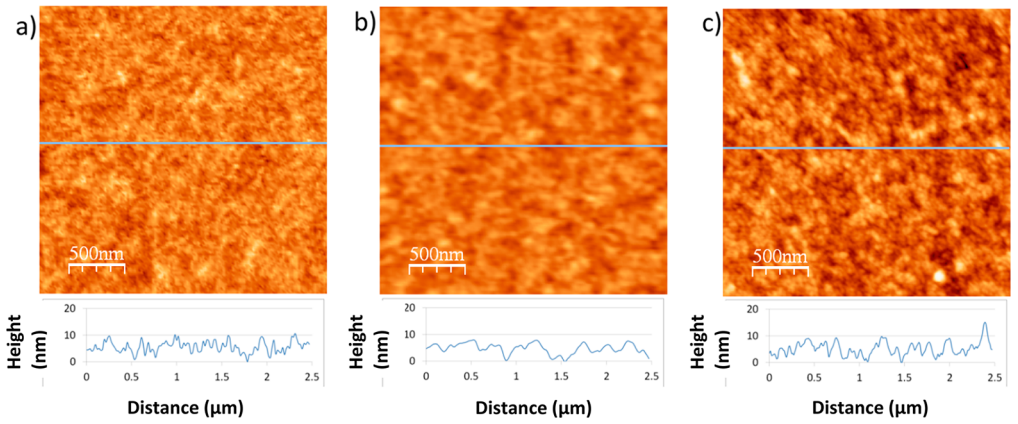

Figure 1. Atomic force microscope images illustrating the change in grain size for (a) water-VPP PEDOT, (b) standard-VPP PEDOT, and (c) DMF-VPP PEDOT films. The image area is 2.5 × 2.5 μm, with the scale bar being 500 nm.

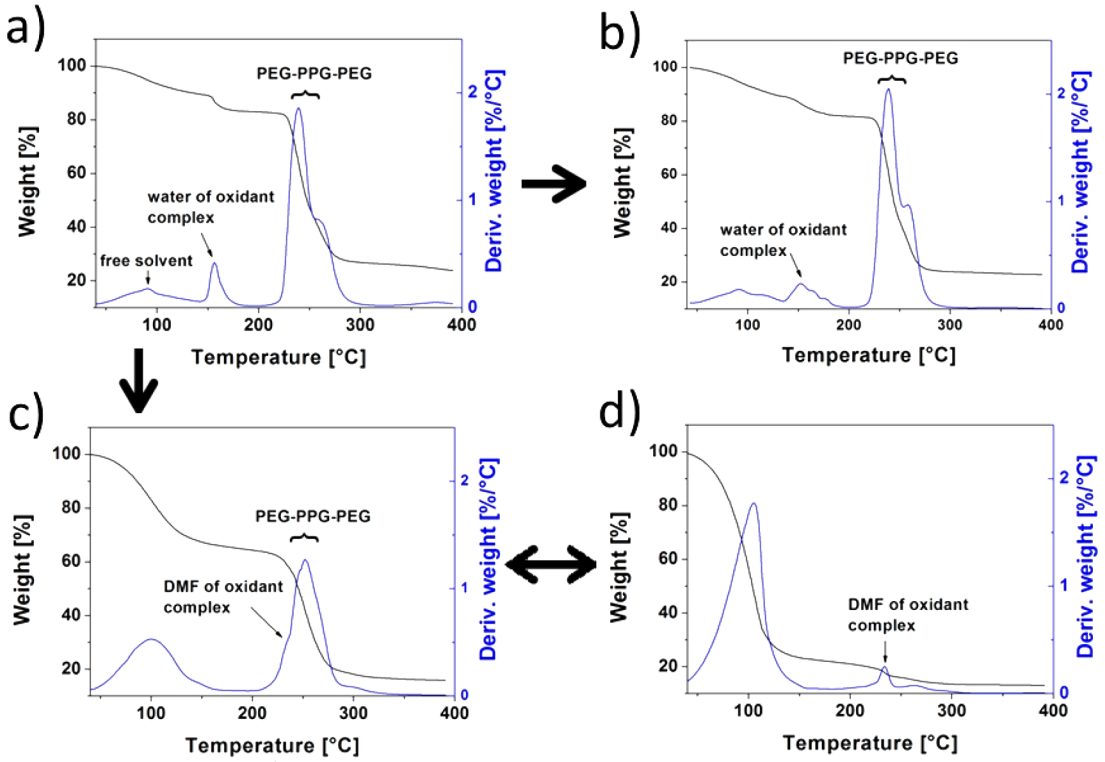

Figure 2. Thermogravimetric analysis of the conditioned oxidant solutions: (a) the standard oxidant solution showing the free solvent (alcohol and water), bound water, and the triblock copolymer; (b) the oxidant solution with added water, still showing the presence of bound water, albeit with a more complex derivative curve; (c) the oxidant solution with added DMF, showing a significant reduction in bound water; (d) DMF and oxidant (no PEG_{20}-PPG_{70}-PEG_{20}) solution showing the presence of bound DMF.

In order to investigate the effect of manipulating the coordination shell which surrounds the iron center on the polymerization of PEDOT, the first part of this investigation focuses on the addition of DMF and water. This is followed by the effect of other selected ligands on the final film properties. Water and DMF were substituted into the oxidant solution in the range 5−50 wt % of the total liquid weight (butanol plus water or DMF), replacing the butanol solvent. The oxidant solutions were then used to prepare vacuum-VPP PEDOT films as have been previously reported.[2,29] It was observed that with the addition of 50 percent water or DMF, a noticeable impact on PEDOT films resulted. The atomic force microscope (AFM) images presented in Figure 1 highlight how the PEDOT film grain size varied with the two additives compared to the standard oxidant. The addition of water yielded smaller grains (ca. 50 nm), while the addition of DMF produced larger sized grains (ca. 300 nm) when compared to the standard oxidant solution (ca. 200 nm). A cursory examination of the *z*-profiles indicates that the change in grain size has also resulted in higher RMS roughness values in both samples (water ∼2.2 nm, DMF ∼ 2.8 nm, std ∼1.8 nm). Additionally (and with equivalent growth times), the thickness of the PEDOT films changed, with those made with the addition of DMF being much thinner (ca. 40 nm) compared to those made with the addition of water (ca. 200 nm). In summary, the AFM observations show that adding water yields thicker films with smaller grain size, while adding DMF results in thinner film consisting of larger grains. With all other parameters held

constant, the most probable reason for the change in grain size and film thickness is a change in the number of nucleation sites. A greater number of nucleation sites leads to rapid polymerization, resulting in a thicker polymer film of PEDOT with smaller grains, as grain growth is constrained because of crowding by neighboring grains.[29] On the other hand, a reduction in the number of nucleation sites slows the rate of PEDOT film growth, resulting in a thinner polymer, allowing larger grains to form owing to the increase in distance to their nearest neighbors. Thus, it can be concluded that the addition of water results in the formation of more active Fe(III) species that initiate polymerization and act as nucleation sites. This result is in agreement with previous findings which demonstrated the critical role that water plays in the polymerization of VPP PEDOT.[30]

To verify the changes in ligand coordination around the Fe(III) centers, in the oxidant solution, thermogravimetric analysis (TGA) measurements were first performed. In Figure 2, the TGA results show four derivative peaks associated with free solvent at 90−100 °C, coordinated water at ∼160 °C, coordinated DMF at ∼240 °C, and the peak for the tri-block PEG-PPG-PEG at 240−280 °C. The effect of water addition is observed by comparing parts a and b in Figure 2, whereby the coordinated water located at ∼160 °C is shifted down to ∼150 °C with the derivative peak now having a more complex shape, an indication that more than one type of coordination exists. By adding DMF to the oxidant solution, the coordinated water peak is greatly reduced at ∼160 °C with only a small shoulder being present (Figure 2c), with the peak associated with coordinated DMF residing at ∼240 °C (refer to Figure 2d, which has DMF added to the oxidant in the absence of PEG-PPG-PEG). Even at this high wt % of DMF, there is still some bound water as suggested by the small shoulder observed at ∼150 °C (Figure 2c). Combining these observations, one can conclude that (i) the addition of water increases the amount of coordination water and (ii) the addition of DMF decreases the percentage of coordination water within the oxidant solution. Furthermore, DMF is hypothesized to coordinate to the Fe(III) since the derivative peak is located at ∼240 °C, which is well above the boiling point of DMF. Thus, DMF indirectly controls the level of active water coordinated to the Fe(III) within the oxidant film which ultimately controls the amount of nucleation sites during polymerization.

The addition of water or DMF to the oxidant solution yields a change in the color of the solution (see SI Figure S1). UV−visible spectra of these samples are able to provide more detailed information about changes in the oxidant solution. Figure 3 shows three main absorption peaks located at ca. 220 nm, 260 nm, and 340 nm for the three oxidant solutions. A review of the literature indicates that each of these broad peaks is the convolution of many smaller individual components related to different iron complexes.[38−40] A general change, however, in form of the rise of the absorption located at ca. 340 nm, between the highly active water based solution and the DMF based solution with less nucleation activity can be observed. Based on the literature[17,19] dealing with aqueous iron complexes, it can be suggested that the active species in the oxidative polymerization of EDOT are a binuclear hydrated iron complex. The appearance of the broad peak at 340 nm is an indicator that adding DMF results in its contribution to the Fe coordination shell and the formation of new complexes with a smaller energy difference between degenerate d-orbitals and/or removing water from the coordination shell and the

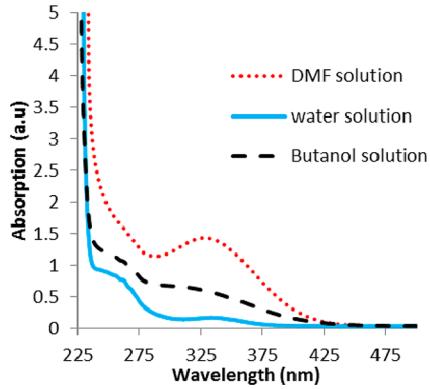

Figure 3. UV−vis spectra for oxidant solutions containing: butanol (i.e. standard solution), added water, and added DMF.

formation of small oligonuclear Fe_xO_y clusters or large Fe_2O_3 species.[38] However, quantifying the exact nature of the changes in the Fe-ligand interaction is beyond the scope of this investigation and not central to the proposed method of controlling the nucleation sites for the polymerization of the conducting polymer. Rather the observations simply confirm that changes in the chemistry of the Fe(III) coordinated compounds have occurred in the oxidant mixture. Running the vacuum-VPP process using oxidant solutions containing different amount of additives (as detailed in SI Table S1) shows that only oxidants that show an absorption peak at 260 nm are able to produce a polymer film. Thus, it can be concluded that the iron complex with this absorption peak is the specie responsible for oxidative polymerization of EDOT.

In order to have a better understanding of the effect of these additives on the redox behavior of the oxidant solution, cyclic voltammetry has been utilized. Figure 4 demonstrates changes

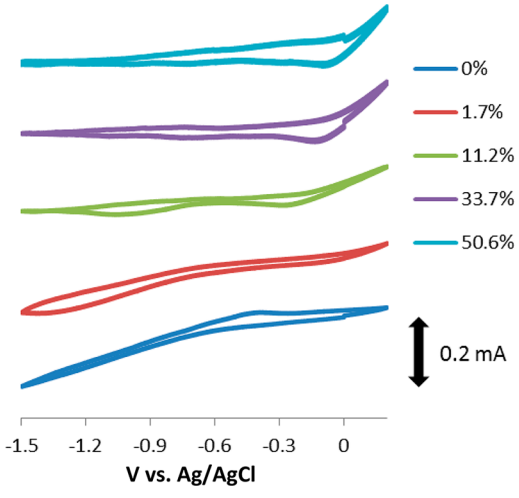

Figure 4. Cyclic voltagram of oxidant solutions containing 0−50 % of coordinating additive (DMSO).

in the cyclic voltagram for oxidant mixtures containing various amounts of coordinating additives (DMSO). It can be seen that an oxidizing specie that starts to reduce at ∼ −0.6 V vs Ag/AgCl exists in the standard oxidant solution. The inclusion of the additive gradually diminishes this redox response and instead a new reduction peak at ∼ −0.1 V appears. Conducting VPP with these oxidant mixtures reveals that only the oxidant solution demonstrating the −0.6 V reduction peak is able to

Table 1. Sheet Resistance (R_s), Thickness, Conductivity (σ), Optical Transmission (% T), Figure of Merit (FoM) and Doping Level of Some PEDOT Sample[a]

	R_s ($\Omega\cdot\square^{-1}$)	T (%)	thickness (nm)	conductivity ($S\cdot cm^{-1}$)	FoM	dop. level (%)
PEDOT	25	68	120	3305	35.5	32.2
water-PEDOT	29	51	202	1707	16.2	31.8
EDTA-PEDOT	473	96.6	22	948	22.2	30.3
EDTA-PEDOT	45.5	63.4	123	1785	16.2	31.8

[a]The detailed recipe of these samples is available in Supporting Information Table S1.

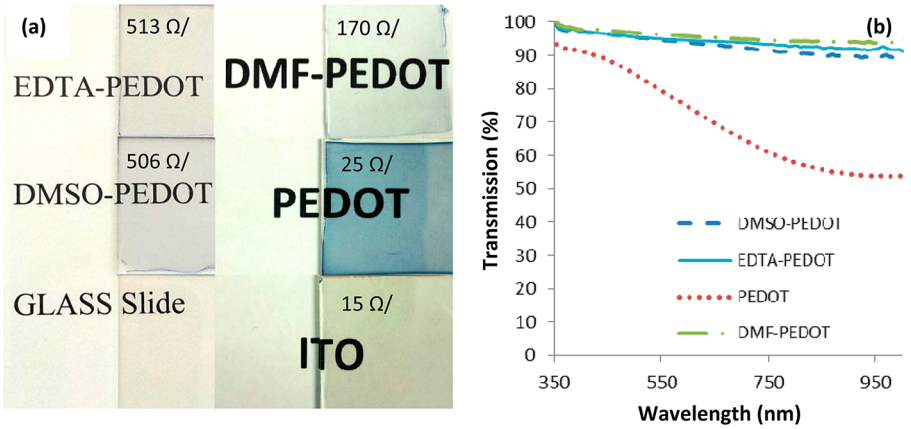

Figure 5. (a) Visual comparison of the optical transparency of the various PEDOT samples compared to bare glass slide and commercially available ITO and (b) the transmission in the visible spectrum for the PEDOT samples. Note the % T values are normalized with respect to the bare glass substrate.

polymerize PEDOT. This can be correlated with the observed changes in the absorbance peaks from UV–vis. Therefore, it can be put forward that oxidizing species exist within the oxidant having a UV–vis absorption peak at 260 nm and a reduction potential of −0.6 V vs Ag/AgCl. From TGA, UV–vis, and CV results, it can be concluded that the addition of these additives can indeed manipulate the coordination of ligands around the iron center, leading to a change in its effective reactivity. It is this manipulation of the Fe(III) coordination shell that ultimately provides a level of control over the nucleation of the forming polymer during vacuum-VPP and hence results in films which are thinner yet robust and conductive.

Based on this initial observation, it was anticipated that the same effect could be observed by adding other aprotic coordinating solvents such as DMSO or NMP or a chelating ligand such as EDTA. In order to test the samples based on these additives, different concentrations were prepared and the resulting PEDOT films' sheet resistance, thickness, and optical transmission were measured. Table S1 in Supporting Information provides results of these measurements and the detailed formulation used for the preparation of these thin films. Table 1 provides a snapshot of the properties of 4 PEDOT film examples. The results show that the introduction of these additives causes a loss of conductivity from ca. ∼3000 $S\cdot cm^{-1}$ down to 400–2000 $S\cdot cm^{-1}$ but enables control over the resultant film thickness, in the range 16–180 nm. The observed loss in PEDOT film conductivity indicates that changing the oxidant chemistry not only changes the morphology and thickness, but it also affects the electrical properties of the films. The conductivity of ICPs is linked to many parameters such as conjugation length, doping level, morphology, etc. Additionally, the interaction between electron rich ligands (e.g. amines) with the positive charge residing on the PEDOT can also result in a loss of conductivity.[31] In order to test if the addition of these additives does indeed change the properties of the polymer films by influencing the doping level, the S2p peak in the XPS spectra was investigated. Supporting Information Figure S2 shows a typical S2p peak deconvoluted into its components. It can be observed (Table 1) that the introduction of various additives has no appreciable effect on the doping level of the samples. The most significant effect, albeit small, is observed for the EDTA-PEDOT sample. This is rationalized by the interaction of the primary amine groups of EDTA with the dislocated positive charges along the PEDOT backbone that results in de-doping of PEDOT that interrupts the conjugated double bonds producing a decrease in conductivity.[31] The N1s peak in the XPS survey spectrum of this sample confirms the presence of nitrogen on this film, while such a peak is absent in the other films (Supporting Inforamtion Figure S3).

The optical transmission of the produced films is within the range of 52% to 98%. Converting transmittance to absorbance and plotting absorbance as a function of thickness (Supporting Information Figure S4) produced a linear relationship (i.e. follows Beer–Lambert law). This indicates that all the films have a similar absorption cross section and density, which consequently yields the same overall light absorption properties. In Figure 5a, a visual comparison is made between selected thin PEDOT films, the "standard" PEDOT, and ITO. While the appearances of the PEDOT samples have a characteristic blue hue, as opposed to the yellow hue of ITO, their transparencies are comparable to the ITO sample. The transmission spectra of the PEDOT samples within the visible range (Figure 5b) provides a quantified demonstration of the effect of the coordinating additives.

Using eq 1, the FoM for these polymers was calculated to be within the range 12–25. A review of the literature in this area shows that the FoM value for graphene (a promising TCE

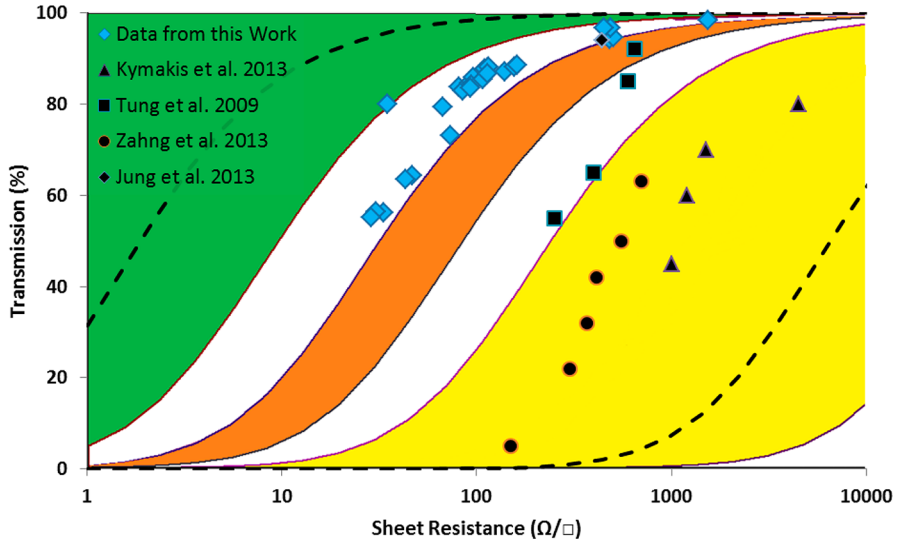

Figure 6. Optical transmission vs sheet resistance for industry demand (green), graphene prepared via reduction of graphene oxide (RGO; yellow), and chemical vapor deposition (CVD; orange) methods. The area between two dashed lines presents the variety of ICP technologies based on PEDOT. The data points in blue are the samples presented in this work (Supporting Information Table S1). The colored bands are based on data reported in ref 19; the example data points for graphene based transparent electrodes are based on data from refs 7, 8, 10, and 11.

alternative and competitor to PEDOT) lays in the range from 0.022 to 25.[7,8,10,11,19] To put these values into context, Figure 6 shows optical transmission versus sheet resistance for PEDOT samples and graphene, prepared using different methodologies (the graph is generated based on data reported in refs 7, 8, 10, 11, 14, 15, and 19). Comparing the values shows that not only does the vacuum-VPP PEDOT, in the presence of a PEG-PPG-PEG tri-block copolymer, meets the requirements for TCE application, but manipulating the iron coordination shell can also be used to modify the optical transparency of the films. It should be noted that although the introduction of these coordinating additives results in some conductivity loss, the resulting thin PEDOT films remain close to industry standards compared to the touted graphene replacement. The main focus of this article, however, is on the opto-electrical properties of these materials, specifically as TCEs, and that conducting polymers and graphene each have functional properties (e.g. electrochemical, catalytic, chemical) that may render one a preferred candidate over the other, when considering them as the active material in a given device.

The stability of PEDOT films under ambient conditions was investigated by monitoring their optical transmission and sheet resistance over 15 days. The optical transmission of all samples changed within the range of ±2% of their respective starting value. However, the sheet resistance of samples rose by ~10 % within the first week after preparation and then stabilized (Supporting Information Figure S5). This observation is in agreement with the previously reported results by Madl et al.[13] Such a loss in conductivity can be attributed to the effect of humidity.[13] Especially in the case of vacuum-VPP polymerized PEDOT, the presence of poly(ethylene glycol) within the polymer film may make it more hygroscopic. The important result here is that the changes in the properties of samples made using coordinating additives is comparable to PEDOT samples based on the standard oxidant solution. Thus, manipulating the oxidant solution using these additives has no detrimental effect on properties of PEDOT.

4. CONCLUSION

Conducting polymer coatings with FoM of 12−25 and thicknesses down to less than 20 nm have been prepared. These robust films out-perform the opto-electrical properties of previously reported graphene films, and approach the accepted industry standard for TCEs applications. Combining the results from TGA, UV−vis, and CV suggests that the addition of aprotic polar solvents or chelating agents to the oxidant mixture has the ability to manipulate the properties of the Fe(III) complex. Doing so allows for control over the nucleation and growth of the conducting polymer during VPP to achieve thin robust films with high FoM values. This method overcomes the shortcomings of alternate approaches for preparation of thin films of conducting polymers, thus creating transparent, conducting polymer thin films that are mechanically robust enough to withstand the post processing steps despite being <20 nm thick.

■ ASSOCIATED CONTENT

Ⓢ Supporting Information

Table S1: composition of various oxidant solutions. Figures S1−S5: oxidant color change, XPS results, optical absorbance vs thickness and change in sheet resistance vs time, respectively. This material is available free of charge *via* the Internet at http://pubs.acs.org

■ AUTHOR INFORMATION

Corresponding Author

*E-mail: rick.fabretto@unisa.edu.au.

Notes

The authors declare no competing financial interest.

■ REFERENCES

(1) Bae, S.; Kim, H.; Lee, Y.; Xu, X.; Park, J.-S.; Zheng, Y.; Balakrishnan, J.; Lei, T.; Ri Kim, H.; Song, Y. I.; Kim, Y.-J.; Kim, K. S.; Ozyilmaz, B.; Ahn, J.-H.; Hong, B. H.; Iijima, S. *Nat. Nanotechnol.* **2010**, *5*, 574−578.

(2) Fabretto, M. V.; Evans, D. R.; Mueller, M.; Zuber, K.; Hojati-Talemi, P.; Short, R. D.; Wallace, G. G.; Murphy, P. J. *Chem. Mat.* **2012**, *24*, 3998−4003.
(3) Wu, J.; Agrawal, M.; Becerril, H. A.; Bao, Z.; Liu, Z.; Chen, Y.; Peumans, P. *ACS Nano* **2009**, *4*, 43−48.
(4) Park, H.; Howden, R. M.; Barr, M. C.; Bulović, V.; Gleason, K.; Kong, J. *ACS Nano* **2012**, *6*, 6370−6377.
(5) Park, J.; Lee, S.; Song, P. *Met. Mater. Int.* **2007**, *13*, 475−478.
(6) Yang, W.; Liu, Z.; Peng, D.-L.; Zhang, F.; Huang, H.; Xie, Y.; Wu, Z. *Appl. Surf. Sci.* **2009**, *255*, 5669−5673.
(7) Jung, Y. U.; Oh, S.-i.; Choa, S.-H.; Kim, H.-K.; Kang, S. J. *Curr. Appl. Phys.* **2013**, *13*, 1331−1334.
(8) Kymakis, E.; Savva, K.; Stylianakis, M. M.; Fotakis, C.; Stratakis, E. *Adv. Funct. Mater.* **2013**, *23*, 2742−2749.
(9) Becerril, H. A.; Mao, J.; Liu, Z.; Stoltenberg, R. M.; Bao, Z.; Chen, Y. *ACS Nano* **2008**, *2*, 463−470.
(10) Zhang, Q.; Wan, X.; Xing, F.; Huang, L.; Long, G.; Yi, N.; Ni, W.; Liu, Z.; Tian, J.; Chen, Y. *Nano Res.* **2013**, *6*, 478−484.
(11) Tung, V. C.; Chen, L.-M.; Allen, M. J.; Wassei, J. K.; Nelson, K.; Kaner, R. B.; Yang, Y. *Nano Lett.* **2009**, *9*, 1949−1955.
(12) Lindell, L.; Burquel, A.; Jakobsson, F. L. E.; Lemaur, V.; Berggren, M.; Lazzaroni, R.; Cornil, J.; Salaneck, W. R.; Crispin, X. *Chem. Mater.* **2006**, *18*, 4246−4252.
(13) Madl, C. M.; Kariuki, P. N.; Gendron, J.; Piper, L. F. J.; Jones, W. E., Jr. *Synth. Met.* **2011**, *161*, 1159−1165.
(14) Alemu Mengistie, D.; Wang, P.-C.; Chu, C.-W. *J. Mater. Chem. A* **2013**, *1*, 9907−9915.
(15) Alemu, D.; Wei, H.-Y.; Ho, K.-C.; Chu, C.-W. *Energy Environ. Sci.* **2012**, *5*, 9662−9671.
(16) Xia, Y.; Ouyang, J. *ACS Appl. Mater. Interfaces* **2012**, *4*, 4131−4140.
(17) Xia, Y.; Ouyang, J. *J. Mater. Chem.* **2011**, *21*, 4927−4936.
(18) Tao, C. S.; Jiang, J.; Tao, M. *Sol. Energy Mater. Sol. Cells* **2011**, *95*, 3176−3180.
(19) De, S.; Coleman, J. N. *ACS Nano* **2010**, *4*, 2713−2720.
(20) Lee, W. H.; Suk, J. W.; Lee, J.; Hao, Y.; Park, J.; Yang, J. W.; Ha, H.-W.; Murali, S.; Chou, H.; Akinwande, D.; Kim, K. S.; Ruoff, R. S. *ACS Nano* **2012**, *6*, 1284−1290.
(21) Ellmer, K. *Nat. Photonics* **2012**, *6*, 809−817.
(22) Gupta, R.; Kulkarni, G. U. *ACS Appl. Mater. Interfaces* **2012**, *5*, 730−736.
(23) Forrest, S. R. *Nature* **2004**, *428*, 911−918.
(24) Berson, S.; De Bettignies, R.; Bailly, S.; Guillerez, S. *Adv. Funct. Mater.* **2007**, *17*, 1377−1384.
(25) Saleh, M.; Park, Y. S.; Baumgarten, M.; Kim, J. J.; Müllen, K. *Macromol. Rapid Commun.* **2009**, *30*, 1279−1283.
(26) Brooke, R.; Evans, D.; Dienel, M.; Hojati-Talemi, P.; Murphy, P.; Fabretto, M. *J. Mater. Chem. C* **2013**, *1*, 3353−3358.
(27) Zhu, Z.-T.; Mabeck, J. T.; Zhu, C.; Cady, N. C.; Batt, C. A.; Malliaras, G. G. *Chem. Commun.* **2004**, 1556−1557.
(28) Badre, C.; Marquant, L.; Alsayed, A. M.; Hough, L. A. *Adv. Funct. Mater.* **2012**, *22*, 2723−2727.
(29) Evans, D.; Fabretto, M.; Mueller, M.; Zuber, K.; Short, R.; Murphy, P. *J. Mater. Chem.* **2012**, *22*, 14889−14895.
(30) Mueller, M.; Fabretto, M.; Evans, D.; Hojati-Talemi, P.; Gruber, C.; Murphy, P. *Polymer* **2012**, *53*, 2146−2151.
(31) Hojati-Talemi, P.; Evans, D.; Fabretto, M. *Chem. Mat.* **2013**, *25*, 1837−1841.
(32) Bennett, M. J.; Cotton, F. A.; Weaver, D. L. *Acta Crystallogr.* **1967**, *23*, 581−586.
(33) Scarrow, R. C.; Raymond, K. N. *Inorg. Chem.* **1988**, *27*, 4140−4149.
(34) Marlin, D. S.; Olmstead, M. M.; Mascharak, P. K. *Inorg. Chem.* **1999**, *38*, 3258−3260.
(35) Ngwack, B.; Sigg, L. *Geochim. Cosmochim. Acta* **1997**, *61*, 951−963.
(36) Hua, G.; Zhang, Q.; McManus, D.; Slawin, A. M. Z.; Woollins, J. D. *Dalton Trans.* **2006**, 1147−1156.
(37) Subramanian, P.; Clark, N. B.; Spiccia, L.; MacFarlane, D. R.; Winther-Jensen, B.; Forsyth, C. *Synth. Met.* **2008**, *158*, 704−711.
(38) Kumar, M. S.; Schwidder, M.; Grünert, W.; Brückner, A. *J. Catal.* **2004**, *227*, 384−397.
(39) Lopes, L.; de Laat, J.; Legube, B. *Inorg. Chem.* **2002**, *41*, 2505−2517.
(40) Stefánsson, A. *Environ. Sci. Technol.* **2007**, *41*, 6117−6123.
(41) Rollick, K. L.; Kochi, J. K. *J. Am. Chem. Soc.* **1982**, *104*, 1319−1330.